Catalysis Today 147S (2009) S51–S57

Contents lists available at ScienceDirect

Catalysis Today

journal homepage: www.elsevier.com/locate/cattod

Mesostructured TUD-1 supported molybdophosphoric acid (HPMo/TUD-1) catalysts for n-heptane hydroisomerization

Dapeng Liu, Xian-Yang Quek, Shuangquan Hu, Lusi Li, Hui Min Lim, Yanhui Yang *

School of Chemical and Biomedical Engineering, Nanyang Technological University, Singapore 637459, Singapore

ARTICLE INFO

Article history:
Available online 30 July 2009

Keywords:
TUD-1
HPMo
Bifunctional catalysts
n-Heptane hydroisomerization

ABSTRACT

Mesoporous molecular sieves TUD-1 (Technische Universiteit Delft) supported molybodophosphoric acid (HPMo) catalysts with various loadings of active HPMo component (10–50 wt.%) were prepared and characterized using X-ray diffraction, thermal analysis, infrared spectroscopy, Raman spectroscopy and temperature-programmed desorption of ammonia. The characterization results revealed that HPMo was highly dispersed over TUD-1 support in the samples with HPMo loading no more than 30 wt.%. The supported catalysts were tested in the hydroisomerization of n-heptane at atmosphere pressure in the temperature range of 200–350 °C. The optimal HPMo content for the reaction was found around 30 wt.%. High isomer selectivity and superior long-term stability were observed over this catalyst.

1. Introduction

Catalytic hydroconversion of straight chain alkanes is of great importance for petroleum refining industry because of the increasingly stringent environmental regulations and fuel specifications. The branched alkane isomers are preferable components to boost the octane level of gasoline and to improve the low-temperature performance of diesel or lubricating oils [1–3]. Paraffin hydroisomerization is generally conducted over bifunctional catalysts consisting of noble metal particles supported on an acid support. During the reaction, the metal sites catalyze hydrogenation/dehydrogenation while the isomerization and/or cracking steps occur on acid centers. Moreover, the presence of noble metal also helps in alleviating the catalyst deactivation by hydrogenating coke precursors. As the reaction proceeds via carbenium ions as intermediates, other acid catalyzed reactions such as cracking or oligomerization may compete with isomerization [4,5]. Meanwhile, the isomer selectivity is also limited by the thermodynamic equilibrium because the branched alkanes are more favorably generated under lower reaction temperature.

Solid acid materials with high acid strength, such as heteropoly acids (HPA) [6–8], sulfated zirconia [9–11] and tungstated zirconia [12–15] have been explored as catalysts in hydroisomerization. It is of our particular interest to employ the HPA in catalytic application because heteropoly anions based on the Keggin structure have been effectively utilized in acid and oxidation reactions in both heterogeneous and homogeneous systems [16,17]. It is well-recognized that HPAs (e.g., $H_3PW_{12}O_{40}$ and $H_3PMo_{12}O_{40}$) in the solid state are pure Brønsted acid, and the acidity is stronger than many mineral acids and conventional solid acids such as SiO_2–Al_2O_3 and HY zeolites [18]. However, bulk HPAs are nonporous materials with surface area below 10 $m^2\,g^{-1}$, only a few acid sites are accessible to reactants. Incorporating large cations, such as Cs^+, Rb^+ and NH_4^+, may increase the surface area in the order of 150 $m^2\,g^{-1}$ [19,20]. Alternatively, HPA can be supported on acidic or neutral carriers with high surface area, e.g., SiO_2, active carbon and acidic ion-exchange resin with SiO_2 being the most frequently used material [21,22]. It was reported that Pt-promoted $Cs_{2.5}H_{0.5}PW_{12}O_{40}$ was efficient for the isomerization of n-alkane (n = 4, 5, 6, 7) [23–26], the decreased deactivation and cracking were observed after the addition of Pt. The mechanical mixture of Pt/Al_2O_3 and $Cs_{2.5}H_{0.5}PW_{12}O_{40}$ showed better catalytic activity and selectivity than that of $Pt/Al_2O_3 + SO_4^{2-}/ZrO_2$ and Pt/Al_2O_3 + H-ZSM-5 in isomerization of n-pentane, n-hexane and n-heptane [27,26]. Recently, Wang et al. [28] have found a high activity and unique selectivity towards multibranched isoheptanes over Pt-promoted HPW/Zr-MCM-41 catalysts, which reflects the superiority of supporting HPA components over the mesostructured material.

A novel mesostructured silicate TUD-1 (Technische Universiteit Delft) will be used as support in current work. This material can be readily synthesized with surfactant-free method, which is environmental friendly and cost-effective [29]. Particularly, its three-dimensional silicate network, sponge-link structure with a highly tunable surface area, high substrate accessibility, and high stability make it the advantages over other microporous and mesoporous materials [29,30]. These characteristics of TUD-1 combined with the strong acidity of HPAs are expected to show

* Corresponding author. Tel.: +65 6316 8940; fax: +65 6794 7553.
E-mail address: yhyang@ntu.edu.sg (Y. Yang).

0920-5861/$ – see front matter © 2009 Elsevier B.V. All rights reserved.
doi:10.1016/j.cattod.2009.07.017

superior activity in the hydroisomerization of alkanes such as n-heptane.

2. Experimental

2.1. Catalyst preparation

Mesostructured siliceous TUD-1 was synthesized following the method reported by Jansen et al. [29] with tetraethyl orthosilicate (TEOS), triethanolamine (TEA) and tetraethyl ammonium hydroxide (TEAOH) as starting materials. In a typical synthesis, a mixture of TEA and H_2O was added dropwise into TEOS and stirred at room temperature for 30 min. Subsequently, TEAOH was added dropwise while stirring. The final molar ratio of the synthesis mixture is $1SiO_2$:1TEA:0.3TEAOH:$11H_2O$. The mixture was aged at room temperature for 24 h, dried at 100 °C for 24 h, followed by hydrothermal treatment in a Teflon-lined stainless steel autoclave for 8 h. The resulting product was calcined at 600 °C for 10 h in air to remove the organic template.

TUD-1 supported molybdophosphoric acid (HPMo) catalysts were prepared by wet impregnating siliceous TUD-1 in HPMo solution with an appropriate HPMo content. The loading of HPMo was regulated at 10–50 wt.%. Platinum was loaded with H_2PtCl_6 solution by wet impregnation to get the Pt content of 0.5 wt.%. After impregnation, the catalysts were dried at 80 °C overnight and calcined at 350 °C for 4 h in air. Hereafter, the supported catalysts are referred to as *x*HPMo (*x* = 10, 20, 30, 40, 50) for clarity.

2.2. Catalyst characterizations

Thermal analysis (TG-DTA) was performed on a SDT Q600 instrument with a heating rate of 10 °C/min from room temperature to 800 °C under air flow. Nitrogen physisorption isotherms were measured on a Quantachrome Autosorb-6B instrument at −196 °C. Samples were previously evacuated at 250 °C overnight and the pore size distribution was calculated with BJH model from the desorption branch of the N_2 adsorption–desorption isotherms. X-ray diffraction (XRD) patterns were acquired on a Bruker D8Focus diffractometer using Cu Kα radiation at 40 kV and 40 mA with a resolution of 0.02° (2θ). Infrared (IR) spectra were recorded on a PerkinElmer Spectrum One FT-IR spectrometer at room temperature with KBr pellets (1800–400 cm^{-1}, resolution of 4 cm^{-1}, and 32 scans). Raman spectra were collected in the range of 1200–200 cm^{-1} at room temperature on a Renishaw Raman spectrometer with a Nd:YAG laser source under room temperature. The acidity of the supported catalysts was investigated via temperature-programmed desorption of ammonia (NH_3-TPD) on a Quantachrome Autosorb-1C instrument. The samples were pretreated at 300 °C under flowing helium followed by NH_3 adsorption at 100 °C. After removing the physisorbed NH_3, TPD analysis was carried out between 100 and 650 °C at a ramping rate of 8 °C/min under flowing helium, the desorbed gas was detected with a thermal conductivity detector. The released NH_3 was absorbed in 0.01 M sulfuric acid and subsequently titrated with 0.01 M sodium hydroxide.

2.3. Catalytic tests

The catalytic experiments were carried out in a fixed bed continuous down-flow reactor. Approximately 0.5 g of the catalyst was loaded into the quartz tube and pretreated under H_2 flow at 300 °C for 2 h under atmospheric pressure. n-Heptane was fed into the reactor using a high-pressure pump. An on-line gas chromatograph equipped with a flame ionization detector (FID) and a HP-PONA capillary column was used to analyze the reactant and products. The reaction conditions used in this work are weight hourly space velocity (WHSV) of 0.8 h^{-1}, H_2/n-C_7 molar ratio of 26, atmosphere pressure, and reaction temperatures ranging from 200 to 350 °C and 300 °C for varying temperature and stability test, respectively.

3. Results and discussion

3.1. Thermal analysis

The thermal stability of the calcined supported catalysts was evaluated by TG-DTA and the results are presented in Fig. 1. The

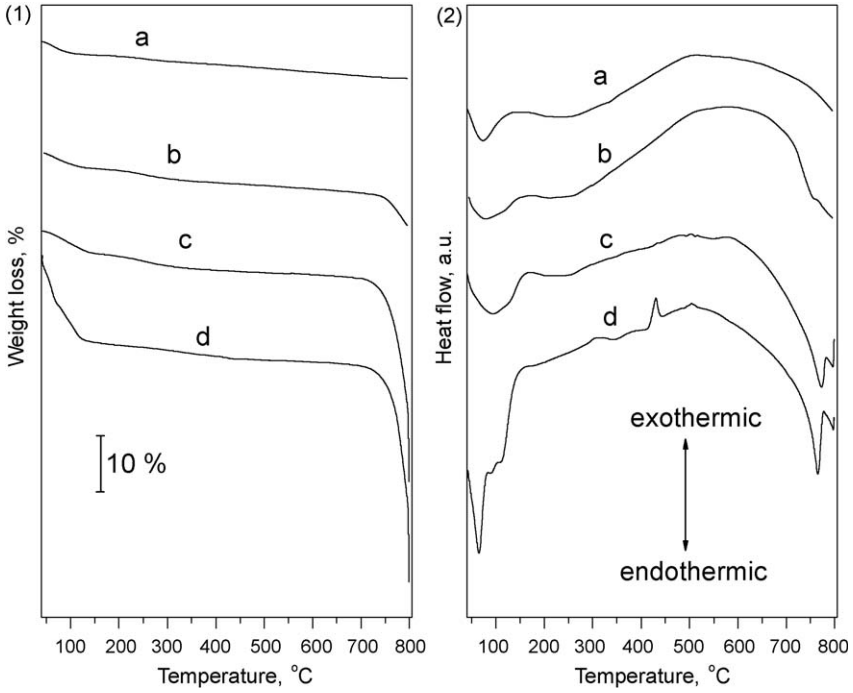

Fig. 1. TG-DTA profiles of TUD-1 supported HPMo catalysts and bulk HPMo: (a) 10HPMo, (b) 30HPMo, (c) 50HPMo and (d) HPMo.

weight loss increases with the loading of HPMo and the sequence is 10HPMo/TUD-1 (6.8%) < 30HPMo/TUD-1 (13.0%) < 50HPMo/TUD-1 (45.1%) < HPMo (58.7%).

All the TUD-1 supported HPMo catalysts show a relatively flat profile of weight loss in contrast with bulk HPMo (Fig. 1(1)). This delayed gradual loss is likely due to the inclusion of the hydrated HPMo inside the mesopores of TUD-1 support. The DTA curve of bulk HPMo exhibits three endothermic peaks (65, 90, 111 °C) below 200 °C, which correspond to the loss of crystallization and/or adsorbed water, forming anhydrous heteropolyoxo compound [31,32]. At high temperature (~400 °C), the formation of constitution water is proposed, which originates from acidic protons and the oxygen belonging to the Keggin units [32]. The exothermic peak at 431 °C and broad shoulder around 510 °C may be due to the decomposition of $HPMo_{12}O_{39}$ and crystallization of MoO_3 [33,34]. It is observed from Fig. 1(2) that all TUD-1 supported catalysts show endothermic peaks below 100 °C which is caused by the loss of adsorbed water in carriers or water of crystallization in HPMo. No visible exothermic peak appears from 400 to 600 °C suggesting the strong interaction between HPMo and TUD-1 support. In contrast to the bulk HPMo, the thermal stability of HPMo substantially increases after TUD-1 immobilization, which coincides with previous reports [35,36].

3.2. Nitrogen physisorption

Nitrogen sorption was used to confirm the structural properties of TUD-1 supported catalysts and the results are shown in Fig. 2(1). All isotherms exist a sharp step at intermediate relative pressure (P/P_o) of 0.5–0.8, representing the mesostructured character of TUD-1 is well-retained after HPMo loading. All the samples give type IV adsorption isotherms with a hysteresis loop. The surface area calculated by the BET method is 645 m^2/g for TUD-1, and decreases gradually with increasing the HPMo loadings, 582, 425 and 293 m^2/g for 10HPMo, 30HPMo and 50HPMo, respectively. The same trend is also seen for pore volume, 1.1, 1.0, 0.79 and 0.52 ml/g for TUD-1, 10HPMo, 30HPMo and 50HPMo, respectively. All TUD-1 samples exhibit pore diameter between 5.8 and 6.1 nm. A slight shrinkage of pore size can be observed with increasing the HPMo content, which is most likely caused by the decreased interaction between HPMo species and the silica matrix under high HPMo loading.

3.3. XRD analysis

The XRD patterns of calcined supported HPMo samples along with bulk HPMo are presented in Fig. 2(2). All the water of crystallization has been removed after calcination at 350 °C, whereas, the constitution water was still retained. For all the supported HPMo catalysts, a broad peak centered at ca. 2θ of 23° originates from the amorphous nature of pore wall of TUD-1 support. Most of the diffractions observed in the non-supported HPMo disappear, and the crystal phases of MoO_3 are absent for all the samples as well. As the loading of HPMo increases, the diffraction peaks of HPMo appear accompanied by the increase of their peak intensities, implying that high dispersion of HPMo can only be achieved with the HPMo loading no more than 30 wt.%.

3.4. IR spectroscopy

IR spectroscopy was used to gain insight into the molecular nature of the supported catalysts. The IR spectra of supported HPMo samples along with bulk HPMo are shown in Fig. 3(1). The main characteristic bands of the Keggin structure at 1065 cm^{-1} (ν_{as} P–O_a), 962 cm^{-1} (ν_{as} Mo–O_d), 870 cm^{-1} (ν_{as} Mo–O_b–Mo) and 789 cm^{-1} (ν_{as} Mo–O_c–Mo) (O_a, oxygen atom bound to 3Mo atoms and the central P atom; O_b and O_c, bridging oxygen atoms; O_d, terminal oxygen atoms) are observed for the bulk HPMo material, in consistence with the previous report [37]. The above vibrations are also visible over the supported catalysts with HPMo loading no less than 30 wt.% and their corresponding intensities increase with the increase of HPMo content. Besides, the framework bands of TUD-1 support also present for the supported samples. The vibrations at 1087 cm^{-1} and a shoulder at 1220 cm^{-1} are due to the asymmetric stretching vibrations of Si–O–Si bridges, and a small peak at 972 cm^{-1} is assigned to the stretching vibrations of terminal silanol groups (Si–OH) present at defect sites. The structural information of the Keggin unit of HPMo can still be observed in spite of some spectra regions partly overlapped with those bands of TUD-1 framework vibrations.

3.5. Raman spectroscopy

Raman technique is a useful characterization tool to observe the Keggin structures present in HPAs. The Raman spectra of HPMo supported catalysts and bulk HPMo are given in Fig. 3(2). Raman spectrum of bulk HPMo shows typical features of the Keggin structure at 994 cm^{-1} (ν_s Mo–O_d), 981 cm^{-1} (ν_{as} Mo–O_d), 907–847 cm^{-1} (ν_{as} Mo–O_b–Mo), 600 cm^{-1} (ν_{as} Mo–O_c–Mo), and 245 cm^{-1} (ν_s Mo–O_a) [37,38]. These characteristic bands of the Keggin units were retained for TUD-1 supported HPMo catalysts; although slight shifts occur for various samples due to the chemical interaction between HPMo species and the TUD-1 surface. Strong broad spectral bands around 925 cm^{-1} are observed for 20HPMo, 30HPMo and 40HPMo samples. This region is generally ascribed to the stretching vibrations of the bridges between two neighboring trimolybdic groups of the Keggin structure, which are rather sensitive to the thermal treatments. The intensified bands suggest the presence of significant dehydration after 350 °C calcination. The occurrence of additional Raman shifts at 819 cm^{-1} and 665 cm^{-1} over 40HPMo and 50HPMo catalysts suggests that MoO_3 species have been formed because a significant proportion of the HPMo species exists in large aggregated particles over these catalysts.

3.6. Temperature-programmed desorption of ammonia

NH_3-TPD is widely used to characterize the acid properties of solid catalysts, providing information on the acid density and acid strength distribution. The TPD profiles of selected catalysts are shown in Fig. 4. Three acid sites of different strengths can be classified according to the desorption temperature of ammonia. The first peak below 300 °C is ascribed to weak acid sites, the peak after 400 °C is assigned to strong acid sites, and the intermediate peak is caused by medium acid sites. Based on the titration results, the total density of acid sites varies according to the following sequence: 10HPMo (0.197) < 40HPMo (0.365) < 30HPMo (0.406) < 50HPMo (0.472). This order is not in agreement with the increase of HPMo loading on TUD-1 support. The decreased acidity of 40HPMo compare to 30HPMo can be attributed to the partial transformation of HPMo to MoO_3 species.

As far as the acid strength is concerned, no strong acid site exists over 10HPMo, medium and strong acid sites form with increasing the HPMo loading. High content of medium acid sites is observed for samples of 40HPMo and 50HPMo, especially the 40HPMo sample possesses the highest content of medium acid sites among all the supported samples. A shift of NH_3 desorption peak of strong acid sites from 440 (50HPMo) to 488 °C (30HPMo) may suggest a slight increase in the acid site strength for 30HPMo. Furthermore, this 30HPMo sample exhibits more weak acid sites (peak at 244 °C) compare to other samples. The complex acidic properties of 40HPMo and 50HPMo samples are mainly associated with the

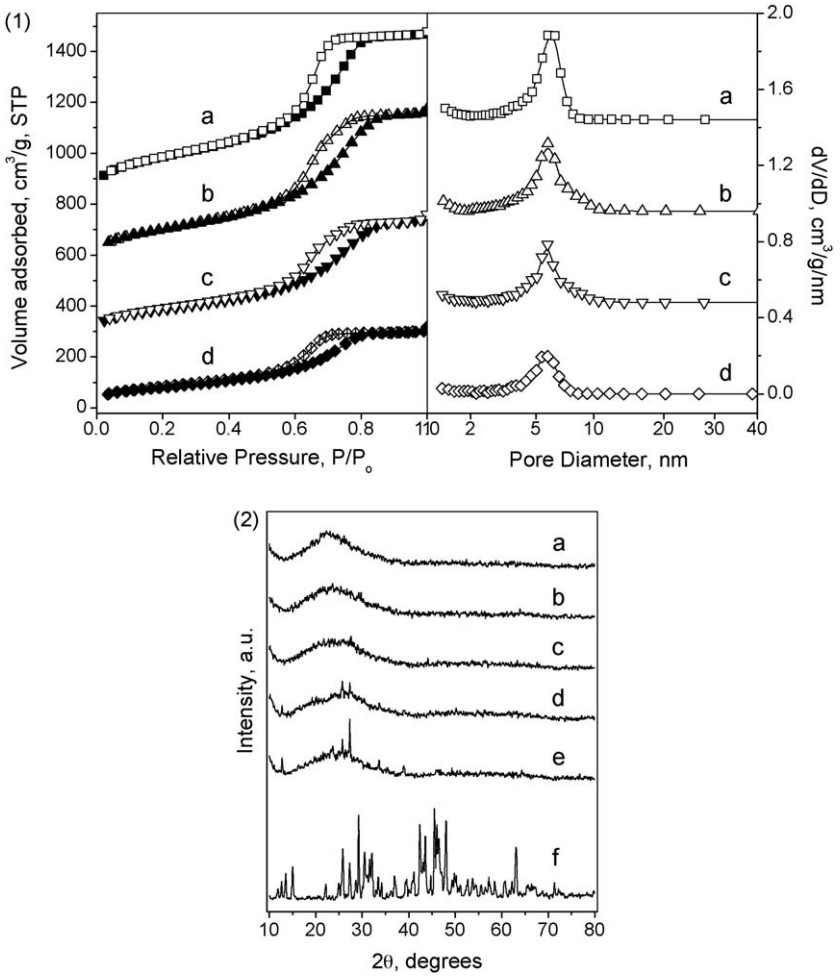

Fig. 2. (1) Nitrogen physisorption results of representative samples: (a) TUD-1, (b) 10HPMo, (c) 30HPMo and (d) 50HPMo; (2) XRD patterns of TUD-1 supported catalysts and bulk HPMo: (a) 10HPMo, (b) 20HPMo, (c) 30HPMo, (d) 40HPMo, (e) 50HPMo and (f) HPMo.

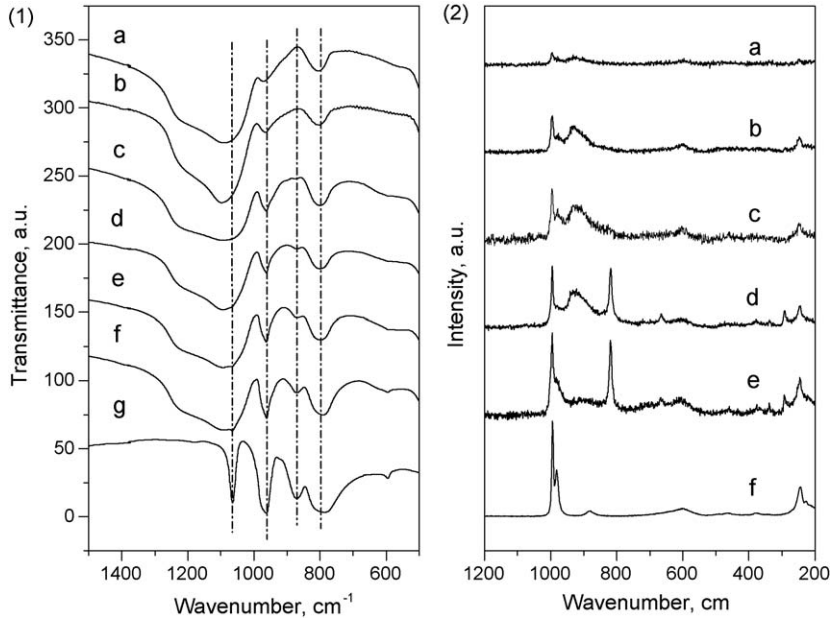

Fig. 3. (1) IR spectra of TUD-1 supported HPMo catalysts and bulk HPMo reference: (a) TUD-1, (b) 10HPMo, (c) 20HPMo, (d) 30HPMo, (e) 40HPMo, (f) 50HPMo and (g) HPMo. (2) Raman spectra of TUD-1 supported catalysts and bulk HPMo reference: (a) 10HPMo, (b) 20HPMo, (c) 30HPMo, (d) 40HPMo, (e) 50HPMo and (f) HPMo.

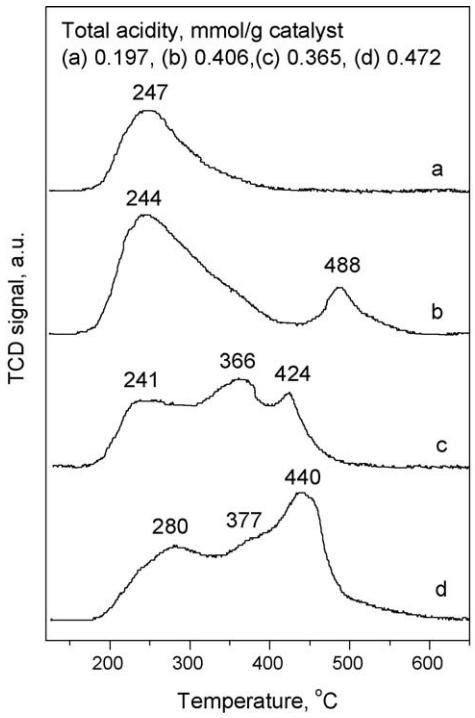

Fig. 4. NH_3-TPD profiles of representative HPMo/TUD-1 catalysts: (a) 10HPMo, (b) 30HPMo, (c) 40HPMo and (d) 50HPMo.

presence of large aggregates of HPMo clusters and the formation of small amount of MoO_3 species.

3.7. Catalytic conversion of n-heptane

Preliminary reaction tests revealed that the catalytic activity was extremely low for bulk HPMo sample. The influence of temperature on the catalytic performance of the supported catalysts with increasing HPMo loading is shown in Fig. 5. Low activity with C_7 conversion below 10% is found as the temperature below 250 °C for all the catalysts (Fig. 5(1)). Nevertheless, C_7 conversion increases rapidly with the temperature afterwards, more significant for 30HPMo, 40HPMo and 50HPMo catalysts. Interestingly, it shows a relatively higher conversion at low-temperature (250–275 °C) for higher HPMo loading catalysts. This can be related to the easier activation of n-C_7 under more acid sites. Both 30HPMo and 50HPMo catalysts exhibit the conversion of C_7 above 70% at the temperatures higher than 300 °C. However, high conversion of C_7 at temperature above 300 °C is accompanied by remarkably low isomer selectivity, which can be clearly observed in Fig. 5(2). Isomer selectivity over 30HPMo catalyst decreases by a factor of 2, from 95% (300 °C) to 48% (350 °C). Under the same condition, isomer selectivity decreases by a factor of 5, from 88.4% to 16.6% over 50HPMo catalyst. The rather low selectivity toward isomers at high temperatures is associated with the strong cracking tendency caused by the consumption of C_7 isomers in the consecutive hydrocracking and the presence of cyclization reaction at high temperature. Fig. 5(2) illustrates that isomer selectivity decreases with HPMo loading, which is substantially consistent with the variation of acid site density and strength. Particularly, the presence of strong acid sites facilitates the cracking reaction under high reaction temperature.

No direct dependence of catalytic activity upon the content of HPMo loading can be observed, considering that the activity of 40HPMo is lower than those of 30HPMo and 50HPMo at temperatures above 300 °C, although C_7 conversion increases regularly as HPMo loading is less than 30 wt.%. In general, it is necessary for the supported catalysts to hold the sufficient acid sites with considerable acid strength for achieving high catalytic activity in isomerization reaction. For 10HPMo and 20HPMo samples, the acid sites are relatively weak and deficient, thus leading to a low catalytic activity. The slightly lower catalytic activity of 40HPMo, in comparison to 30HPMo and 50HPMo, is also closely associated with its relatively low acid density (Fig. 4). Both 30HPMo and 50HPMo catalysts possess high activity, however, 50HPMo gives lower isomer selectivity, implying that total acid sites, especially the strong acid centers over 50HPMo catalyst, are excessive. For 30HPMo catalyst, the density and acid strength of acid sites are moderate. Furthermore, HPMo species with Keggin structures are better dispersed over TUD-1 surface in comparison

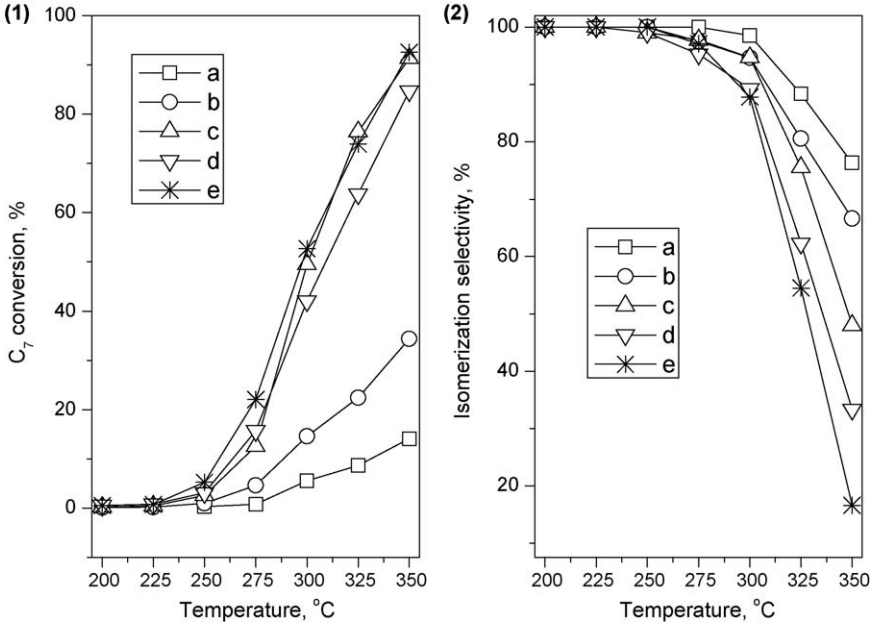

Fig. 5. (1) Conversion of n-C_7 and (2) isomer selectivity vs. temperature over (a) 10HPMo, (b) 20HPMo, (c) 30HPMo, (d) 40HPMo and (e) 50HPMo.

Table 1
Product selectivities (%) at 300 °C during n-C_7 hydroconversion over selected samples.

Catalyst	30HPMo	40HPMo	50HPMo
Conversion (%)	49.5	42.1	52.7
Methane	0.0	0.0	0.0
Ethane	0.1	0.2	0.2
Propane	1.9	4.1	4.7
Isobutane	1.4	4.0	4.7
Butane	1.0	1.4	1.5
2-Methylbutane	0.1	0.2	0.2
Pentane	0.2	0.2	0.2
2-Methylpentane	0.1	0.1	0.1
3-Methylpentane	0.0	0.0	0.0
Hexane	0.1	0.1	0.1
2,2-Dimethylpentane	2.8	2.6	2.8
2,4-Dimethylpentane	4.3	4.7	5.0
2,2,3-Trimethylbutane	0.2	0.3	0.3
3,3-Dimethylpentane	1.6	1.5	1.6
2-Methylhexane	35.9	33.7	32.6
2,3-Dimethylpentane	6.7	7.3	7.8
3-Methylhexane	39.9	36.3	35.0
3-Ethylpentane	3.2	2.8	2.7
Methylcyclohexane	0.0	0.2	0.0
Toluene	0.3	0.4	0.6

to 40HPMo and 50HPMo catalysts (Figs. 2(2) and 3). These improved acid characteristics are favorable to maintain a balance between metal and acid sites, thus enhancing catalytic performance of 30HPMo catalyst.

The product distributions measured at 300 °C over 30HPMo, 40HPMo and 50HPMo catalysts are summarized in Table 1. Same types of products are formed over all catalysts, which include generally: (a) isoheptanes (monobranched and dibranched C_7 isomers, and trace amounts of trimethylbutane), (b) cracking products (light hydrocarbons) with carbon number less than 7, and (c) trace amounts of cyclization products, namely, methycyclohexane and toluene. No methane is detected, which implies that the hydrogenolysis reactions occurring over metal sites can be neglected. Isomerization is the main reaction, with 2-methylhexane and 3-metalhexane as primary products and multibranched C_7 isomers occupying only a small fraction. The preferential 3-methylhexane selectivity among monobranched C_7 isomers can be attributed to the absence of diffusion restriction [39]. Larger amount of cracking products are formed over 40HPMo and 50HPMo catalysts, with a higher isobutene/butane ratio than over 30HPMo catalyst, which is indicative of the mismatch of metal/acidity or the lack of close vicinity between them for 40HPMo and 50HPMo catalysts. In cracking products, almost equal amounts of propane and isobutene suggest that 2,2-dimethylpentane and 2,4-dimethylpentane crack predominantly [40].

Considering the better catalytic activity and the higher isomerization selectivity can be achieved over 30HPMo catalyst compared to other catalysts. Meanwhile, at the temperatures above 300 °C, more cracking components and cyclization products, such as methylcyclohexane and toluene, have been formed. The 30HPMo catalyst and 300 °C are selected for further stability evaluation.

The evaluation results of catalytic long-term stability of 30HPMo catalyst are presented in Fig. 6. It shows a considerably stable C_7 conversion with slight fluctuation between 54% and 60%, and a high isomer selectivity (between 92% and 96%). It is evident that 30HPMo catalyst maintains both a stable activity and high selectivity of isomers for the hydroisomerization of C_7. The product distributions are substantially retained during 30 h time-on-stream (TOS). This promising catalytic performance is probably due to the high dispersion of acidic sites over three-dimensional mesostructured TUD-1 support as well as the well-balanced metal sites and acid sites.

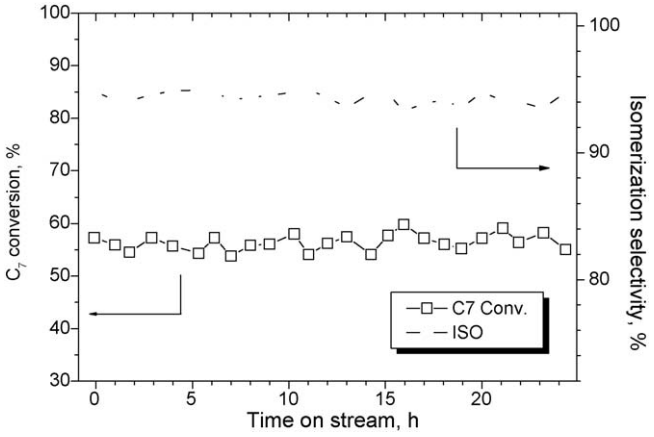

Fig. 6. Catalytic stability of 30HPMo catalyst as a function of time-on-stream.

4. Conclusion

The catalytic properties of mesostructured TUD-1 supported HPMo catalysts for n-C_7 hydroisomerization were investigated. A highly dispersed HPMo catalysts can be prepared with HPMo loading less than 30 wt.%. Higher content of HPMo led to the formation of HPMo aggregates and MoO_3 clusters. The high catalytic activity was observed for the catalysts with HPMo loading greater than 30 wt.%. However, only 30HPMo catalyst showed superior isomerization selectivity. More cracking products were formed over 40HPMo and 50HPMo catalysts due to the presence of a large proportion of relatively strong acid sites. The stable catalytic activity and high isomer selectivity were confirmed in 30 h TOS evaluation. The superior catalytic performance of HPMo/TUD-1 mainly originated from the high dispersion of acid sites on mesostructured TUD-1 support and the well-presented synergetic interaction between Pt metallic clusters and acid sites.

Acknowledgements

The authors thank AcRF tier 2 (M45120006 ARC 13/07) for providing funding support.

References

[1] H. Weyda, E. Köhler, Catal. Today 81 (2003) 51.
[2] I.E. Maxwell, W.H.J. Stork, Stud. Surf. Sci. Catal. 137 (2001) 747.
[3] S.J. Miller, Stud. Surf. Sci. Catal. 84 (1994) 2319.
[4] A. Corma, J. Planelles, J. Sanchez-Marin, F. Thomas, J. Catal. 93 (1985) 30.
[5] M. Guisnet, N.S. Gnep, Appl. Catal. A: Gen. 146 (1996) 33.
[6] Y. Liu, G. Koyano, M. Misono, Top. Catal. 11/12 (2000) 239.
[7] N. Essayem, Y. Ben Tâarit, P.Y. Gayraud, G. Sapaly, C. Naccache, J. Catal. 203 (2001) 157.
[8] B.B. Bardin, R.J. Davis, Top. Catal. 6 (1998) 77.
[9] X. Song, A. Sayari, Catal. Rev. Sci. Eng. 38 (1996) 329.
[10] S. Rezgui, R.E. Jentoft, B.C. Gates, Catal. Lett. 51 (1998) 229.
[11] V. Adeeva, H.Y. Liu, B.Q. Xu, W.H.M. Sachtler, Top. Catal. 6 (1998) 61.
[12] M. Hino, K. Arata, J. Chem. Soc., Chem. Commun. (1987) 1259.
[13] S.R. Vaudagna, R.A. Comelli, N.S. Fígolií, Appl. Catal. 164 (1997) 265.
[14] E. Iglesia, D.G. Barton, S.L. Soled, S. Miseo, J.E. Baumgartner, W.E. Gates, G.A. Fuentes, G.D. Meitzner, Stud. Surf. Sci. Catal. 101 (1996) 533.
[15] S.V. Filimonova, A.V. Nosov, M. Scheithauer, H. Knözinger, J. Catal. 198 (2001) 89.
[16] T. Okuhara, N. Mizuno, M. Misono, Adv. Catal. 41 (1996) 113.
[17] I.V. Kozhevnikov, Chem. Rev. 98 (1998) 171.
[18] N. Mizuno, M. Misono, Chem. Rev. 98 (1998) 199.
[19] J.B. Moffat, J. Mol. Catal. 52 (1989) 169.
[20] J.L. Bonardet, K. Carr, J. Fraissard, G.B. McGarvey, J.B. McMonagle, M. Seay, J.B. Moffat, Advanced Catalysts and Nanostructured Materials, Elsevier, Amsterdam, 1996, p. 395 (Chapter 15).
[21] K. Nowinska, R. Fiedorow, J. Adamiec, J. Chem. Soc., Faraday Trans. 87 (1991) 749.
[22] I.V. Kozhevnikov, Catal. Rev. Sci. Eng. 37 (1995) 311.
[23] K. Na, T. Okuhara, M. Misono, J. Catal. 170 (1997) 96.
[24] Y. Liu, K. Na, M. Misono, J. Mol. Catal. A: Chem. 141 (1999) 145.

[25] C. Travers, N. Essayem, M. Delage, S. Quelen, Catal. Today 65 (2000) 355.
[26] Y. Liu, G. Koyano, M. Misono, Top. Catal. 11/12 (2000) 239.
[27] Y.Y. Liu, G. Koyano, K. Na, M. Misono, Appl. Catal. A 166 (1998) L263.
[28] J.A. Wang, X.L. Zhou, L.F. Chen, L.E. Norena, G.X. Yu, C.L. Li, J. Mol. Catal. A: Chem. 299 (2009) 68.
[29] J.C. Jansen, Z. Shan, L. Marchese, W. Zhou, N. van der Puil, T. Maschmeyer, J. Chem. Soc. Chem. Commun. (2001) 713.
[30] X.-Y. Quek, Q. Tang, S. Hu, Y. Yang, Appl. Catal. A 361 (2009) 130.
[31] H. Atia, U. Armbruster, A. Martin, J. Catal. 258 (2008) 71.
[32] B.K. Hodnett, J.B. Moffat, J. Catal. 88 (1984) 253.
[33] R.I. Maksimovskaya, G.M. Maksimov, G.S. Litvak, Russ. J. Chem. Bull. Int. Ed. 25 (2003) 103.
[34] C. Rocchiccioli-Deltcheff, A. Aouissi, M.M. Bettahar, S. Launay, M. Fournier, J. Catal. 164 (1996) 16.
[35] K.M. Rao, R. Gobetto, A. Iannibello, A. Zecchina, J. Catal. 119 (1989) 512.
[36] S. Kasztelan, E. Payen, J.B. Moffat, J. Catal. 125 (1990) 45.
[37] C. Rocchiccioli-Deltcheff, M. Fournier, R. Franck, Inorg. Chem. 22 (1983) 207.
[38] S. Damyanova, J.L.G. Fierro, Chem. Mater. 10 (1998) 871.
[39] D. Liu, S. Hu, R. Lau, A. Borgna, G.L. Haller, Y.H. Yang, Chem. Eng. J. 151 (2009) 308.
[40] G.E. Gianetto, G.R. Perot, M. Guisnet, Ind. Eng. Chem. Prod. Res. Dev. 25 (1986) 481.